

RESEARCH REPORT

Myc is dispensable for cardiomyocyte development but rescues *Mycn*-deficient hearts through functional replacement and cell competition

Noelia Muñoz-Martín¹, Rocío Sierra¹, Thomas Schimmang², Cristina Villa del Campo^{1,*} and Miguel Torres^{1,*}

ABSTRACT

Myc is considered an essential transcription factor for heart development, but cardiac defects have only been studied in global *Myc* loss-of-function models. Here, we eliminated *Myc* by recombining a *Myc* floxed allele with the *Nkx2.5Cre* driver. We observed no anatomical, cellular or functional alterations in either fetuses or adult cardiac *Myc*-deficient mice. We re-examined *Myc* expression during development and found no expression in developing cardiomyocytes. In contrast, we confirmed that *Mycn* is essential for cardiomyocyte proliferation and cardiogenesis. Mosaic *Myc* overexpression in a *Mycn*-deficient background shows that *Myc* can replace *Mycn* function, recovering heart development. We further show that this recovery involves the elimination of *Mycn*-deficient cells by cell competition. Our results indicate that *Myc* is dispensable in cardiomyocytes both during cardiogenesis and for adult heart homeostasis, and that *Mycn* is exclusively responsible for cardiomyocyte proliferation during heart development. Nonetheless, our results show that *Myc* can functionally replace *Mycn*. We also show that cardiomyocytes compete according to their combined *Myc* and *Mycn* levels and that cell competition eliminates flawed cardiomyocytes, suggesting its relevance as a quality control mechanism in cardiac development.

KEY WORDS: Heart development, Transcription factor, Proliferation, Apoptosis, Cell competition, Mouse

INTRODUCTION

Myc transcription factors promote cell growth and division, being essential for proliferation in healthy tissues and tumours. *Myc* proteins belong to the basic helix-loop-helix-domain family and exert their functions mainly by regulating transcription. There are three members of the *Myc* family of transcription factors in mammals: *Myc*, *Mycn* and *Mycl*. All three transcripts show spatially restricted patterns during post-implantation embryonic development (Zimmerman et al., 1986). Deregulation of these genes has been linked with tumour formation and cell growth.

Myc expression is required for normal embryonic development in mammals, displaying widespread expression from early stages of development, and becoming regionally restricted starting at embryonic day (E) 7.5. Global *Myc* knockout embryos die between E9.5 and E10.5, showing defects in heart, pericardium and neural

tube, and delay or failure of embryo turning (Davis et al., 1993). Strong *Myc* overexpression in transgenic mice enhances myocyte proliferation during heart development, promoting cardiac hyperplasia, which suggested the idea of an essential role of *Myc* in cardiomyocyte growth and proliferation during development (Jackson et al., 1990). In contrast, strong *Myc* overexpression during postnatal life leads to premature cardiomyocyte hypertrophy (Machida et al., 1997; Xiao et al., 2001) and heart-specific deletion of *Myc* prevents hypertrophic growth in response to hemodynamic, pharmacological (Zhong et al., 2006) and cold-induced (Bello Roufai et al., 2007) hypertrophy. *Myc* mRNA levels in whole hearts decrease in correlation with the transition from hyperplastic to hypertrophic growth (Schneider et al., 1986) and *Myc* is not expressed in adult cardiomyocytes under normal conditions but becomes strongly activated following hypertrophic stimuli (Izumo et al., 1988; Pollack et al., 1994), which suggests that the physiological function of *Myc* in postnatal cardiomyocytes is restricted to the hypertrophic response to a challenge. In agreement with this idea, *Myc* deletion in cardiomyocytes of unchallenged adult mouse hearts does not lead to cardiac function alterations (Zhong et al., 2006).

Further experiments in a model of moderate overexpression of *Myc* produced a very different set of results. Mild *Myc* overexpression in a cellular mosaic fashion does not produce overt phenotypical alterations during embryonic development or adult life, but induces the phenomenon of cell competition, by which cells with enhanced anabolism eliminate and replace neighbours without altering tissue homeostasis (Claveria et al., 2013; Claveria and Torres, 2016). In cardiac-specific models of *Myc* mosaic overexpression at moderate levels, *Myc*-enhanced cardiomyocytes trigger the elimination of neighbouring wild-type cardiomyocytes both during development and in the adult heart (Villa del Campo et al., 2014, 2016).

The changes induced by moderate *Myc* overexpression in cardiomyocytes remain within homeostatic limits both during development and in the adult heart (Villa del Campo et al., 2014). Notably, in these experiments, *Myc*-enhanced adult hearts are not prone to hypertrophy but display a mild hyperplastic phenotype (Villa del Campo et al., 2014). The contrast of these results with those obtained by strong overexpression of *Myc* in transgenic mice (Machida et al., 1997; Xiao et al., 2001) suggests that the effects of *Myc* overexpression depend on the levels induced.

Although the results obtained in overexpression experiments suggest a role for *Myc* during cardiomyocyte development, there are no studies reporting developmental cardiac-specific deletion of *Myc*. Furthermore, the conditional deletion of *Myc* in the blood/endothelial lineage produces heart defects similar to those observed in complete *Myc* elimination (He et al., 2008), raising the possibility that the cardiac defects observed in the global mutant do not result from a primary function in cardiomyocytes. In contrast, *Mycn* is essential for cardiomyocyte development in conditional deletion

¹Cardiovascular Development Program, Centro Nacional de Investigaciones Cardiovasculares, CNIC, 28029 Madrid, Spain. ²Instituto de Biología y Genética Molecular, Universidad de Valladolid y Consejo Superior de Investigaciones Científicas, 47003, Valladolid, Spain.

*Authors for correspondence (mtorres@cnic.es; cristina.villa@cnic.es)

 M.T., 0000-0003-0906-4767

models (Harmelink et al., 2013) whereas *Mycl* expression and mutant phenotypes do not affect the heart (Hatton et al., 1996). *Myc* and *Mycn* show high sequence and structure homology and this translates into a highly conserved function, as exemplified by full rescue by *Mycn* of the *Myc* global knockout in a knock-in replacement mouse model (Malynn et al., 2000).

Mycn global mutants die *in utero* between E10.5 and E11.5, displaying smaller size and hypoplastic heart (Charron et al., 1992; Moens et al., 1993; Sawai et al., 1993; Stanton et al., 1992), a phenotype that is reproduced in a cardiomyocyte-specific deletion of *Mycn* using a *cTnT-Cre* driver (Harmelink et al., 2013). *Mycn* is required for ventricular wall morphogenesis through its role in regulating compact layer cardiomyocyte growth, proliferation and maturation. The defects in heart growth were attributed exclusively to the reduction in proliferation and not to increased cell death (Harmelink et al., 2013).

Here, we studied the role of *Myc* during heart development, the ability of *Myc* to rescue *Mycn* deficiency during cardiogenesis and the involvement of cell competition and cardiomyocyte replacement in this rescue. We report the absence of *Myc* expression or function in developing cardiomyocytes and the ability of *Myc*-expressing cardiomyocyte populations to repopulate *Mycn*-deficient hearts and rescue *Mycn* function. Our results indicate that *Mycn* is essential for cardiomyocyte development, but *Myc* is not involved in this process. Nonetheless, *Myc* is able to mimic *Mycn* function, rescue *Mycn*-deficient cells and promote the elimination of *Mycn*-deficient cells to restore a viable heart.

RESULTS AND DISCUSSION

Myc is dispensable for heart development and adult heart homeostasis

To study the role of *Myc* during heart development, we conditionally deleted *Myc* in mice using the *Nkx2.5-Cre* strain, which drives widespread Cre-mediated recombination in cardiac precursors from around E8.0 (Stanley et al., 2002). *Nkx2.5-Cre*-mediated recombination is complete in cardiomyocytes and affects a large part of endocardial (Stanley et al., 2002) and epicardial (Zhou et al., 2008) precursors. Embryos resulting from elimination of *Myc* function in cardiac progenitors (cKO-*Myc*) (*Myc*^{fllox/fllox}; *Nkx2.5-Cre*^{tg/tg}) were viable and did not display any phenotypic abnormality (Fig. 1A). cKO-*Myc* mice reached adulthood in the expected proportions (Table S1) and presented normal cardiac morphology (Fig. 1A).

Measurements of heart weight revealed no significant differences in size between cKO-*Myc* homozygous, heterozygous and wild-type hearts (Fig. 1B). The density of cardiomyocyte nuclei was similar between cKO-*Myc* homozygous, heterozygous and wild-type hearts (Fig. 1C,D), indicating no alterations in cardiomyocyte size or number.

To assess the function of cKO-*Myc* hearts, we performed echocardiographic assays on 10-week-old adult mice. No significant differences were found between groups in ejection fraction and fractional shortening parameters, indicating that the function of cKO-*Myc* hearts is not affected by the loss of *Myc* (Fig. 1E). Overall, cKO-*Myc* hearts display normal morphology and function and, therefore, our data indicate that *Myc* function in the *Nkx2.5-Cre*⁺ lineages is dispensable for heart formation and adult heart homeostasis.

Myc is not expressed in developing cardiomyocytes

The results obtained could be explained by lack of *Myc* function during cardiomyocyte development or by compensation of a

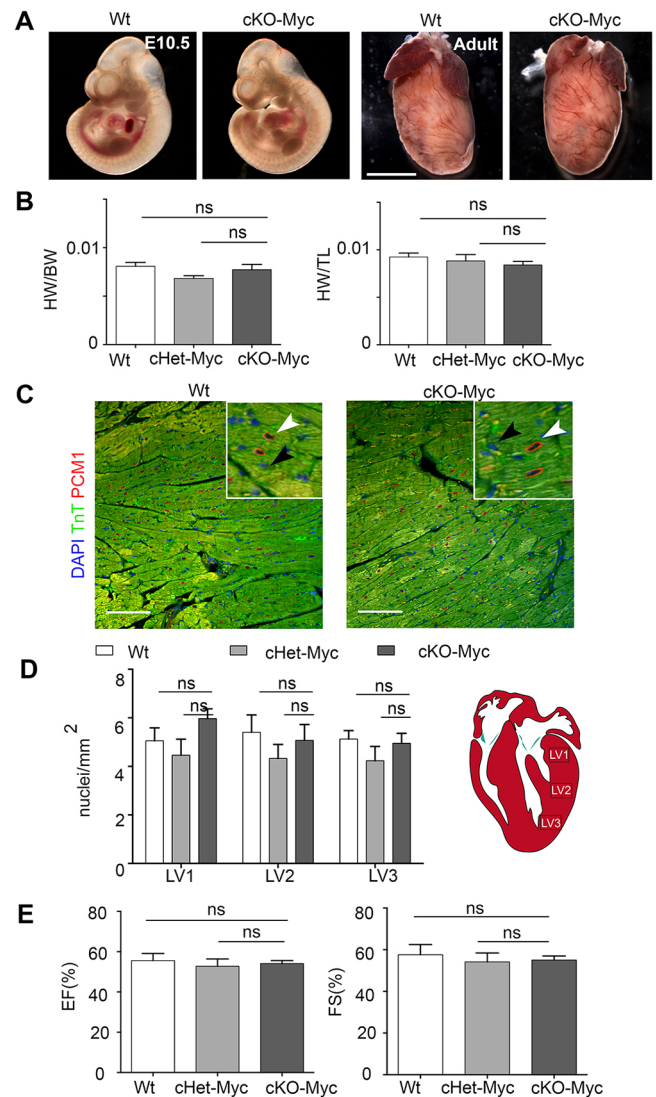


Fig. 1. *Myc* deletion in the *Nkx2.5* lineage. (A) Left: Whole-mount E10.5 wild-type (Wt) and *Mycn*^{fllox/fllox};*Nkx2.5-Cre*^{tg/tg} (cKO-*Myc*) embryos. Right: Whole-mount Wt and cKO-*Myc* adult hearts. (B) Heart/body weight (HW/BW) and heart weight/tibia length (HW/TL) ratios in 10-week-old animals. (C) Confocal images from sections of adult hearts stained with anti-PCM1 (red) and anti-TnT (green). Insets show magnification of cardiomyocyte (white arrow) and non-cardiomyocyte (black arrow) nuclei in heart sections, as detected with PCM-1 antibody. (D) Quantification of cardiomyocyte nuclei per area in three different regions of the left ventricle. Location of the regions within the left ventricle is identified in the schematic as LV1, LV2 and LV3. (E) Ejection fraction (EF) and fractional shortening (FS) measured by echocardiography in adult mice. Data in C,E,F are mean±s.e.m.; ns, not significant ($P>0.05$). $n=3-8$ mice/condition. Scale bars: 500 μ m (A); 100 μ m (C).

putative *Myc* function by *Mycn*. *Myc* RNA expression has been reported by northern blot in mid-gestation samples from whole myocardium (Jackson et al., 1990; Schneider et al., 1986) and *Myc* protein expression has been reported by western blot from whole adult myocardium (Zhong et al., 2006). Here, we performed *in situ* hybridization (ISH) to determine which cells express *Myc* during myocardial development. In agreement with previous reports (Uslu et al., 2014), *Myc* mRNA was expressed at E9.5 in the neural tube, branchial arches, cephalic regions and other non-cardiac tissues (Fig. 2A). At this stage, *Myc* mRNA was not detected in the heart tube, but within the cardiogenic region, expression was seen in the

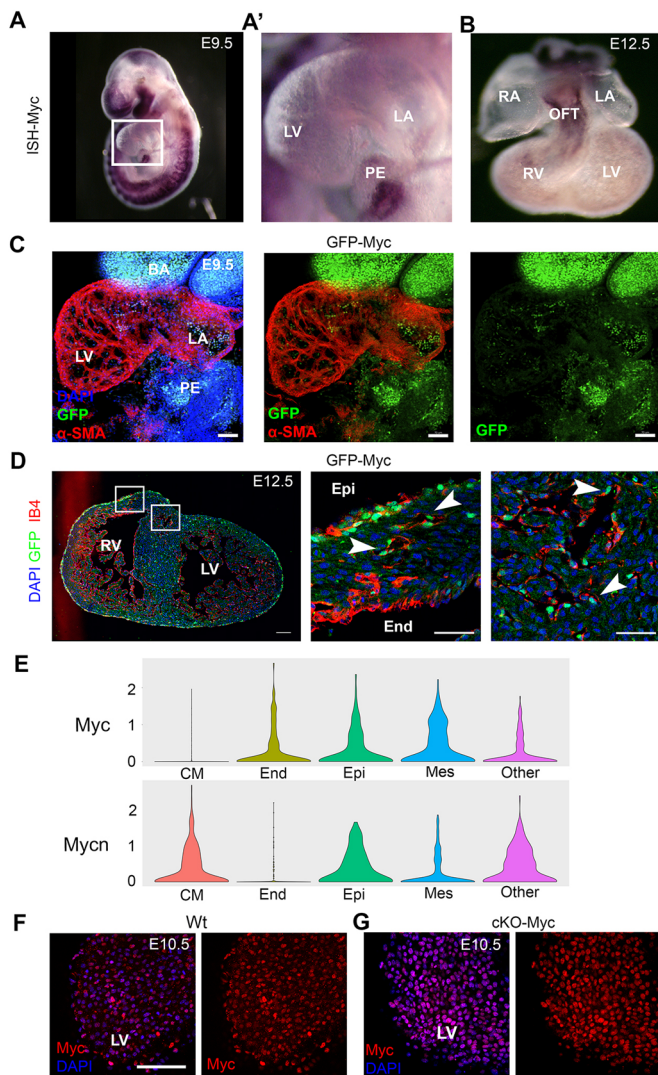


Fig. 2. Myc is not detected in cardiomyocytes during heart development. (A,A') Whole-mount *Myc* ISH of an E9.5 wild-type embryo, with detail of the heart in A' (magnification of the boxed area in A). (B) Whole-mount *Myc* ISH of an E12.5 wild-type embryonic heart. (C) Confocal section of a whole-mount E9.5 *GFP-Myc* embryo showing *GFP-Myc* expression and α -SMA immunostaining. (D) Confocal section of an E12.5 *GFP-Myc* heart showing *GFP-Myc* expression and isolectin GS-IB4 (IB4) as an endothelial marker. Middle and right panels show magnification of the boxed areas of the left panel. Arrowheads point to endothelial cells expressing *GFP-Myc*. (E) Violin plots showing *Myc* and *Mycn* mRNA expression in different cardiac cell types at E10.5. The data are a re-analysis of original data by Li et al., 2016. Violin plots show relative cell abundance (x -axis) versus \log_2 of normalized reads (y -axis) for *Myc* or *Mycn* mRNAs. (F,G) Confocal sections of whole E10.5 wild-type (Wt; F) and cKO-*Myc* (G) hearts showing staining for DAPI and *Myc*. BA, branchial arches; CM, cardiomyocytes; End, endocardium (endocardium/endothelium in E); Epi, epicardium; LA, left atria; LV, left ventricle; Mes, mesenchymal cells; OFT, outflow tract; PE, proepicardium; RA, right atria; RV, right ventricle. Scale bars: 70 μ m (C); 100 μ m (D, left); 50 μ m (D, middle and right, and F,G).

proepicardium (Fig. 2A'). Analysis at later stages showed weak *Myc* mRNA detection in the distal outflow tract (OFT) and subepicardium at E12.5 (Fig. 2B). To confirm *Myc* expression in the developing heart, we took advantage of a *GFP-Myc* knock-in reporter line in which endogenous *Myc* protein expression is reported by green fluorescent protein (GFP) fused to the endogenous *Myc* mRNA open reading frame (Huang et al., 2008).

In agreement with our ISH results, *GFP-Myc* expression at E9.5 was strongly detected in the branchial arches and in the proepicardium (Fig. 2C). In the heart tube, no *GFP-Myc* expression was detected in the myocardium, whereas the endocardium displayed a positive signal. Sectioning of *GFP-Myc* E12.5 hearts showed no *GFP-Myc* expression in cardiomyocytes. It was detected in endothelial cells within the myocardium and subepicardium, with endocardial expression mostly absent (Fig. 2D). In addition, we analysed previous data of single cell RNA-seq from developing mouse hearts at stage E10.5 (Li et al., 2016). *Myc* and *Mycn* mRNAs show complementary patterns in the endothelial and cardiomyocyte populations of E10.5 hearts. *Myc* mRNA is strongly present in endothelial cells, but it is not detected in cardiomyocytes, whereas *Mycn* mRNA shows the opposite expression pattern (Fig. 2E). In addition, the mRNAs of both genes are detected in epicardial, mesenchymal and other mixed cell populations (Fig. 2E).

These results contradict our previous characterization of *Myc* protein distribution using an anti-*Myc* antibody in immunofluorescence, in which a clear signal was detected in cardiomyocytes at E10.5 (Villa del Campo et al., 2014). To resolve this contradiction, we repeated the immunofluorescence comparing wild-type and cKO-*Myc* hearts at E10.5 (Fig. 2F,G). Detection of *Myc* expression in wild-type embryos clearly identified a nuclear signal in cardiomyocytes (Fig. 2F). This signal remained unchanged in cKO-*Myc* hearts (Fig. 2G). This result contrasts with the observation that this antibody has been validated for endogenous *Myc* detection in the E6.5 mouse epiblast (Claveria et al., 2013). Although the most plausible explanation for this result is cross-reaction with *Mycn*, which is expressed in developing cardiomyocytes but not in the E6.5 epiblast (Harmelink et al., 2013; Moens et al., 1993), in *Mycn^{fllox/fllox};Nkx2.5-Cre^{tg/WT}* embryos, the signal persisted (Fig. S1), indicating non-specificity of unknown origin.

We conclude that *Myc* does not play a role in cardiomyocyte development because it is not expressed in this lineage and, thus, it does not act redundantly with *Mycn*.

Forced *Myc* expression in a mosaic fashion is sufficient to rescue cKO-*Mycn* cardiac defects

A relevant question is whether the different effects reported for *Myc* overexpression in cardiomyocytes result from *Myc* mimicking *Mycn* function. As mentioned above, *Mycn* can replace *Myc* functions when knocked in to the *Myc* locus (Malynn et al., 2000). Here, we investigated whether *Myc* could replace *Mycn* function in the developing heart. To test this, we used *Myc* overexpression from the Cre-inducible *Rosa26R-iMOS* mosaic system (Claveria et al., 2013). The *iMOS^{TMyc}* allele allows the induction of mild overexpression of *Myc* in a cellular mosaic fashion (Claveria et al., 2013) (Fig. S2A). In this mosaic model, 75% of recombined cells overexpress *Myc* and are reported by EYFP expression, whereas 25% of recombined cells do not overexpress *Myc* and are reported by ECFP expression (Fig. S2). *Mycn^{fllox/fllox};Nkx2.5-Cre^{tg/+}* embryos in which *Mycn* has been conditionally deleted in heart precursors (cKO-*Mycn*) are not viable past E10.5-E11.5 (Fig. 3A, middle), in accordance with the phenotype previously reported for *Mycn* deletion in cardiomyocytes (Harmelink et al., 2013). In contrast, cardiac *Mycn*-deficient littermates in which the *iMOS^{TMyc}* mosaic has been activated (*Mycn^{fllox/fllox};iMOS^{TMyc/+};Nkx2.5-Cre^{tg/+}*) were viable and indistinguishable from *iMOS^{TMyc}* activation on wild-type (*Mycn^{+/+};iMOS^{TMyc/+};Nkx2.5-Cre^{tg/+}*) or *Mycn*-heterozygous (*Mycn^{fllox/+};iMOS^{TMyc/+};Nkx2.5-Cre^{tg/+}*) backgrounds (Fig. 3A, right); both genotypes being phenotypically normal (Villa del Campo et al., 2014; this study). Histological

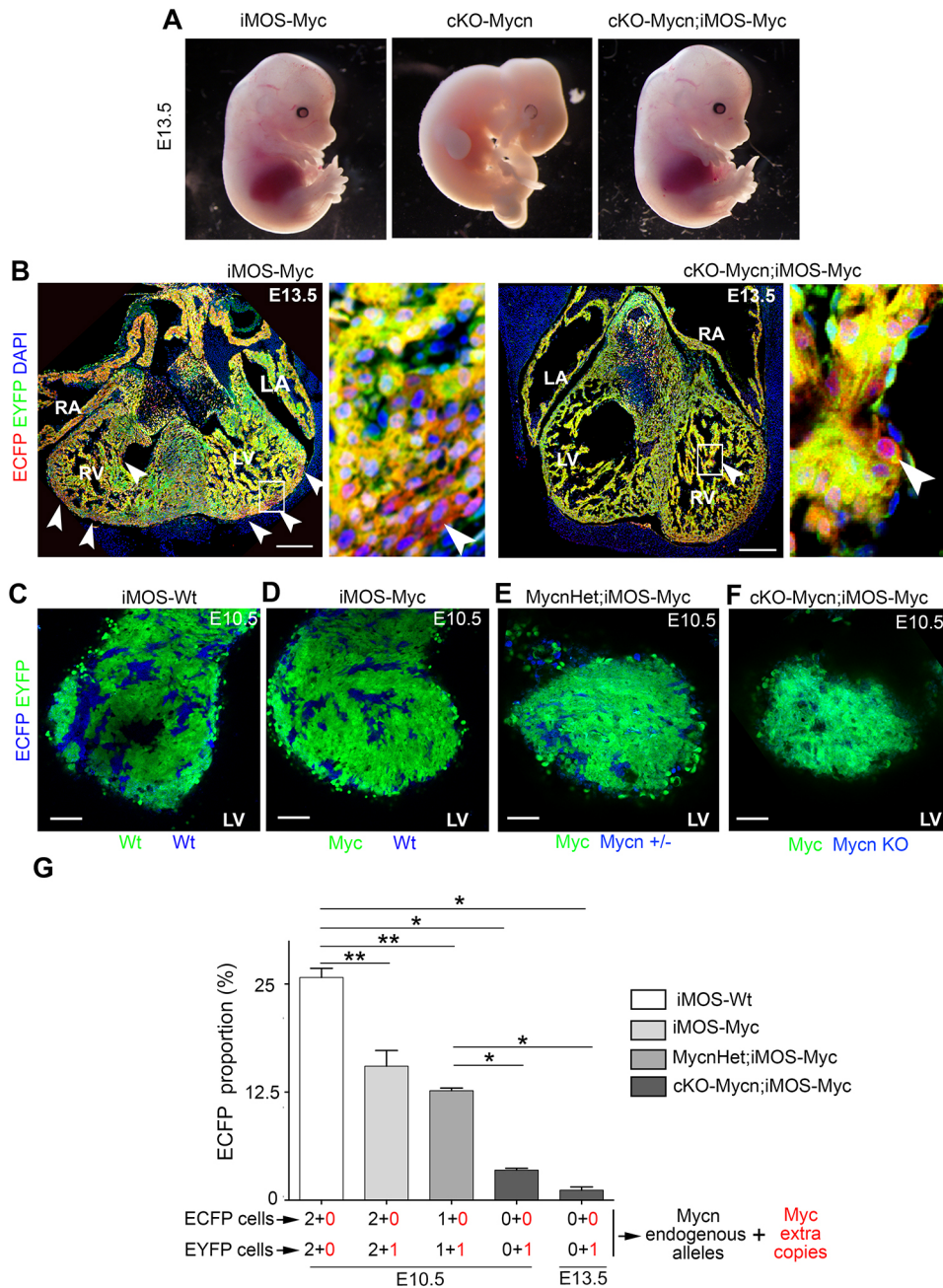


Fig. 3. Myc mosaic overexpression rescues cardiac Mycn deficiency.

(A) Whole-mounts of E13.5 embryos of the following genotypes: *Mycn*^{+/+}; *iMOS*^{T1Myc/+}; *Nkx2.5-Cre*^{tg/+} (iMOS-Myc; left), *Mycn*^{flx/flx}; *Nkx2.5-Cre*^{tg/+} (cKO-Mycn; middle) and *Mycn*^{+/+}; *iMOS*^{T1Myc/+}; *Nkx2.5-Cre*^{tg/+} (cKO-Mycn;iMOS-Myc; right). (B) Confocal section of E13.5 iMOS-Myc and cKO-Mycn hearts, showing EYFP-Myc (yellow) and ECFP-WT (red) cell populations. Arrowheads point to ECFP-positive cells, also displayed in the magnification of boxed areas.

(C-F) Confocal sections of E10.5 iMOS-Wt (*Mycn*^{+/+}; *iMOS*^{WT/+}; *Nkx2.5-Cre*^{tg/+}; C), iMOS-Myc (D), MycnHet;iMOS-Myc (*Mycn*^{flx/flx}; *iMOS*^{T1Myc/+}; *Nkx2.5-Cre*^{tg/+}; E) and cKO-Mycn;iMOS-Myc (F) whole-mount hearts showing endogenous fluorescence from the EYFP (green) and ECFP (blue) cell populations. (G) Percentage of ECFP cells in hearts of iMOS-WT and iMOS-Myc mosaics in the three different *Mycn* backgrounds. The number of *Myc* and *Mycn* combined alleles in each cell population of the different mosaics is shown below the graph. LA, left atria; LV, left ventricle; RA, right atria; RV, right ventricle. *n*=3 cKO-Mycn;iMOS-Myc, *n*=3 cKO-Mycn, *n*=3 iMOS-Myc in *Mycn* heterozygous or wild-type backgrounds. Data in G are mean±s.e.m.; **P*<0.05; ***P*<0.01. Scale bars: 100 μm.

analysis and study of the contribution of the cells recombined by *Nkx2.5-Cre* at E13.5 showed normal contribution of cardiac progenitors to the heart and no morphological alterations were observed in *iMOS*^{T1Myc}-rescued *Mycn*-deficient hearts compared with *iMOS*^{T1Myc} hearts (Fig. 3B). These results indicate that mosaic overexpression of *Myc*, driven by the endogenous *Rosa26* promoter, is enough to functionally replace the loss of *Mycn* expression during heart development.

Cell competition contributes to the rescue of *Mycn*-deficient hearts by stimulating the replacement of deficient cells

The complete phenotypic rescue of cKO-Mycn hearts suggested that, in addition to cell-autonomous replacement of *Mycn* function by *Myc*, some non-cell-autonomous mechanism would operate to either eliminate or rescue the 25% of cells that do not activate *Myc*. To understand which of these mechanisms is at work, we determined

the proportion of ECFP and EYFP cardiomyocyte populations in different genetic configurations. Control *iMOS*^{WT} mosaics expressing only the fluorescent proteins over a wild-type background produce a 25-75% distribution of ECFP and EYFP cardiomyocytes when activated by the *Nkx2.5-Cre* driver (*iMOS*^{WT/+}; *Nkx2.5-Cre*^{tg/+}) (Fig. 3C,G; Fig. S2). The same experiment performed with the *iMOS*^{T1Myc} mosaic reduces the wild-type (ECFP) cell population that does not overexpress *Myc* to 15% from the original 25% (Fig. 3D,G), as a result of cell competition (Fig. 3G) (Villa del Campo et al., 2014). When the *iMOS*^{T1Myc} mosaic was induced over a cardiac *Mycn*-heterozygous background (*Mycn*^{flx/+}; *iMOS*^{T1Myc/+}; *Nkx2.5-Cre*^{tg/+}), the proportion of *Mycn*^{+/-} (ECFP) cardiomyocytes observed in E10.5 hearts was about 12.5% (Fig. 3E,G) whereas when the *iMOS*^{T1Myc} mosaic was induced over a cardiac *Mycn* homozygous deletion (*Mycn*^{flx/flx}; *iMOS*^{T1Myc/+}; *Nkx2.5-Cre*^{tg/+}), the proportion of *Mycn*-KO (ECFP) cells dropped to 3.7% at E10.5 and to 1% at

E13.5 (Fig. 3B,F,G). These results suggest not only the cell-autonomous replacement of *Mycn* by *Myc*, but also that a replacement of *Mycn*-KO cardiomyocytes by *Myc*-overexpressing cardiomyocytes contributes to the rescue of cardiac *Mycn* deficiency.

We next explored the possibility that the elimination of this cell population takes place by cell competition. Elimination of *Mycn*-KO cardiomyocytes when confronted with *Myc*-overexpressing cardiomyocytes was much more efficient than elimination of wild-type or *Mycn*-heterozygous cells, which would fit a scenario in which both *Myc* and *Mycn* act additively to determine cardiomyocyte competition ability. An alternative view would be that *Mycn*-KO cells are not actively eliminated but just diluted out because of their limited ability to proliferate (Fig. 4A,B). To discriminate between these possibilities, we determined the frequency of apoptosis in *Mycn*-KO cardiomyocytes both when in a homotypic environment in *Mycn^{flox/flox};Nkx2.5-Cre^{tg/tg}* hearts, and when confronted with a *Myc*-overexpressing cardiomyocyte population in *Mycn^{flox/flox};iMOS^{T1Myc/+};Nkx2.5-Cre^{tg/tg}* hearts. We found that the apoptotic rate in *Mycn*-KO cardiomyocytes is very low and similar to that found

in wild-type hearts (Fig. 4C,D), which agrees with previous reports (Harmelink et al., 2013). In contrast, *Mycn*-KO cardiomyocytes exposed in mosaic hearts to *Myc*-overexpressing cardiomyocytes, display a strong increase in the frequency of apoptosis (Fig. 4E,F). These results indicate that confrontation with *Myc*-overexpressing rescued cells produces a strong selective apoptotic elimination of *Mycn*-KO cells, which are otherwise viable in a homotypic environment.

Taken together, our results show that *Myc* is not required for heart development in the *Nkx2.5-Cre⁺* lineage and is not detectably expressed in developing cardiomyocytes. Although this excludes a function of *Myc* in cardiomyocytes, the study is not conclusive regarding *Myc* functions in endothelial or epicardial lineages that are not completely affected by *Nkx2.5-Cre* recombination. In the context of previous evidence from endogenous *Myc* expression and function analyses in the adult heart (Jackson et al., 1990; Schneider et al., 1986; Zhong et al., 2006), it is concluded that *Myc* expression and its role in heart physiology are restricted to stress responses during adult life, whereas *Mycn* fully assumes the constitutive roles of the family during

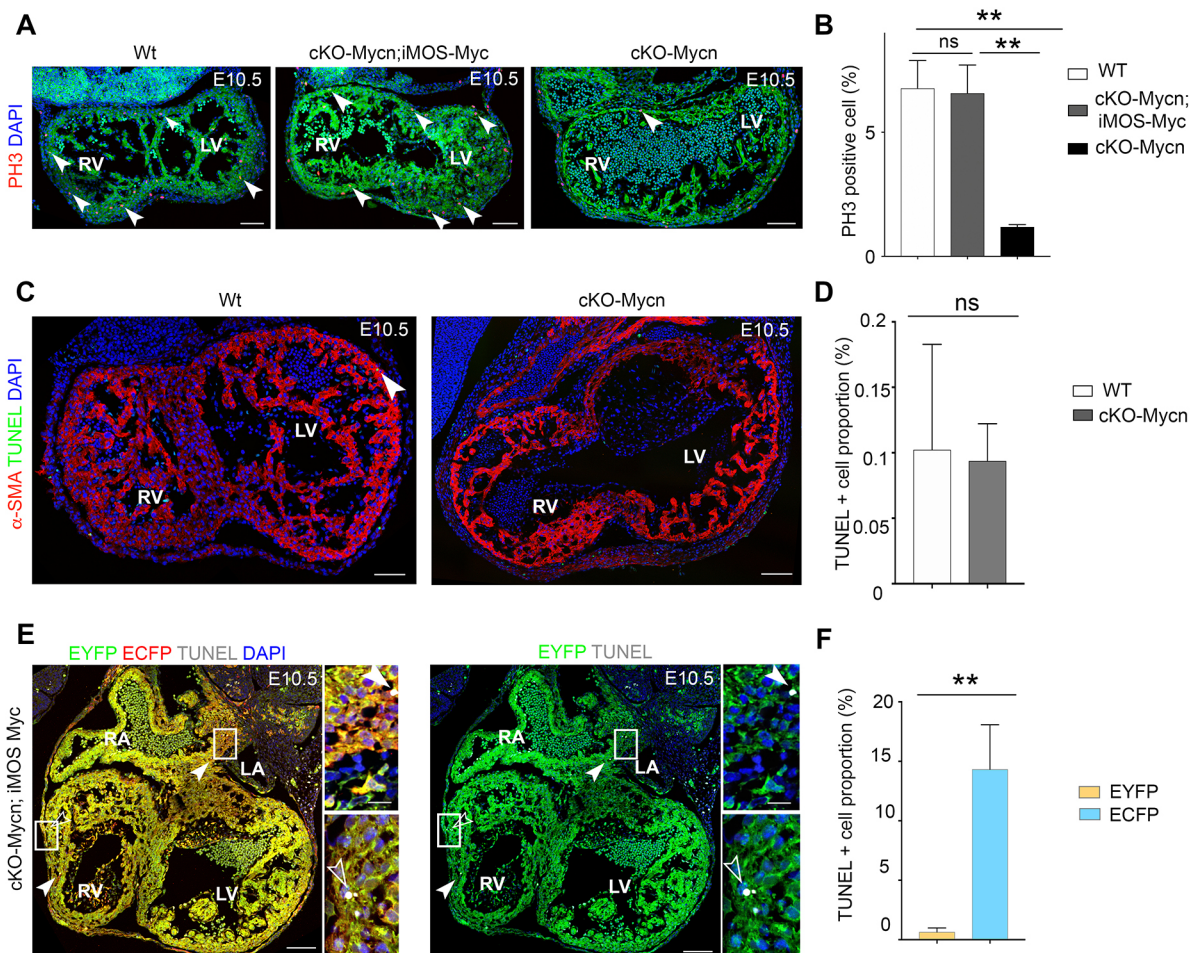


Fig. 4. *Mycn*-deficient cardiomyocytes are eliminated by apoptosis when confronted with *Myc*-overexpressing neighbours. (A) Confocal sections of wild-type (Wt), cKO-Mycn;iMOS-Myc and cKO-Mycn E10.5 hearts (from left to right) showing PH3 staining in red. Arrowheads point to PH3-positive cardiomyocytes. (B) Percentage of PH3-positive cardiomyocytes at E10.5 from the different groups in A. (C) Confocal sections of Wt and cKO-Mycn E10.5 hearts stained by TUNEL and α -SMA immunolabelling. Arrowhead points to TUNEL-positive cardiomyocytes. (D) Percentage of TUNEL-positive cardiomyocytes from the hearts in C. (E) Confocal sections of cKO-Mycn;iMOS-Myc hearts at E10.5 showing EYFP and ECFP populations in the myocardium. Filled arrowheads and top insets (magnifications of the boxed areas) show TUNEL⁺ ECFP⁺ cells. Empty arrowheads and bottom insets show TUNEL⁺ EYFP⁺ cells. (F) Percentage of EYFP- and ECFP-positive cardiomyocytes also positive for TUNEL staining in E10.5 cKO-Mycn;iMOS-Myc hearts. LA, left atria; LV, left ventricle; RA, right atria; RV, right ventricle. $n=3$ cKO-Mycn;iMOS-Myc, $n=4$ cKO-Mycn, $n=3$ iMOS-Myc. Data in B, D, F are mean \pm s.e.m.; * $P<0.05$; ** $P<0.01$; ns, not significant. Scale bars: 100 μ m (A, C, E, main panels); 20 μ m (insets in E).

cardiogenesis. In addition, we show that Myc can replace Mycn functionally during cardiomyocyte development and that cell competition contributes to rescuing heart function by stimulating the elimination of defective cells. This demonstration adds to previous evidence indicating that the developing heart can adapt to the progressive loss of up to 50% of its cardiomyocyte population by compensatory proliferation of the healthy population (Drenckhahn et al., 2008). In contrast to this previously reported model, in which the unhealthy cardiomyocyte population is not eliminated by cell death but just diluted out (Drenckhahn et al., 2008), in the model presented here the unhealthy cell population is not prone to cell death when in isolation but undergoes massive cell death when confronted with a Myc-rescued cardiomyocyte population. These results suggest an endogenous role for cell competition in the correction of contingent defects that may appear in cardiomyocytes during development.

MATERIALS AND METHODS

Mouse strains

iMOS mouse lines have been previously described (Claveria et al., 2013). Homozygous *iMOS* females were mated with males carrying *Nkx2.5-Cre* (Stanley et al., 2002) to generate embryos. The *Mycn* floxed allele has been previously described (Knoepfler et al., 2002), as has been the Myc-GFP reporter (Huang et al., 2008). Mice were genotyped by PCR. All animal procedures were conducted in accordance with applicable institutional guidelines.

ISH

Whole-mount ISH was performed on E9.5 embryos and E12.5 hearts as described previously, using a Myc probe (Claveria et al., 2013)

Confocal microscopy

Histological sections and whole-mount embryos were imaged with a Nikon A1R confocal microscope using 405, 458, 488, 568 and 633 nm wavelengths and 20×/0.75 dry and 40/1.30 oil objectives. Cardiomyocyte nuclei were counted using the ImageJ (NIH; <http://rsb.info.nih.gov/ij>) cell counter. To estimate cardiomyocyte size, the number of nuclei was divided by the myocardial area calculated using ImageJ threshold detection. Areas occupied by EYFP and ECFP cells and EYFP and ECFP cell number were quantified using ImageJ threshold detection and particle analysis tools. ECFP was scored either by direct detection of ECFP or by subtracting the EYFP⁺ area from the anti-GFP⁺ area, when immunostaining was performed.

Measurements in adults

After sacrifice, mice were weighed and hearts were extracted and rinsed in PBS. Hearts were weighed and tibia length of the posterior left leg was measured with a caliper.

Immunofluorescence

Embryos were fixed overnight at 4°C in 2% paraformaldehyde (PFA) in PBS and whole-mount stained or embedded in gelatin and cryosectioned. Embryonic hearts were fixed in 2% PFA overnight at 4°C and stained as whole-mounts. Adult hearts were perfused and fixed in 2% PFA in PBS 24 h at 4°C and paraffin-embedded for sectioning. Primary antibodies used were PC1 (1:100; Sigma, HPA023370), α -SMA (1:500; Sigma, C-6198), Myc (1:300; Millipore, D84C12), goat-anti GFP antibody (1:100; Aacris, R1091P), c-TnT (1:200; Thermo Scientific, Ms-295-P0), IB4-647 (1:500; Thermo Scientific, I32450). Immunofluorescence was performed following standard procedures. Briefly, cryosections were permeabilized with PBT (PBS with 0.5% Triton X-100) and blocked with 10% goat serum, except for anti-GFP, for which 10% donkey serum was used. Primary antibodies were incubated at 4°C overnight and secondaries for 1 h at room temperature. Secondary antibodies used were donkey anti-goat 488 (Invitrogen, A11055), goat anti-rabbit 594 (Invitrogen, A11012), goat anti-mouse 488 (Invitrogen, A11029), goat anti-mouse 594 (Invitrogen, A11005), donkey anti-goat 647 (Invitrogen, A21447), Streptavidin-647 (Invitrogen, A32728). Sections were mounted using Vectashield (Vector Laboratories, H-1000). Terminal deoxynucleotidyl

transferase dUTP nick end labelling (TUNEL) was performed on heart sections using terminal deoxynucleotidyl transferase (TdT) and biotin-16-2-deoxyuridine-5-triphosphate (1:500; Biotin-16-dUTP) (both from Roche), and developed with 647-conjugated streptavidin (1:500; Jackson ImmunoResearch). E9.5 embryos were cleared before whole-mount confocal acquisition using ethyl cinnamate as described by Klingberg et al. (2017).

Echocardiography study

Transthoracic echocardiography was performed blind by an expert operator using a high-frequency ultrasound system (Vevo 2100, Visualsonics, Canada) with a 40-MHz linear probe on a heating platform. Mice were lightly anaesthetized with 0.5-2% isoflurane in oxygen, adjusting the isoflurane to maintain heart rate at 450±50 bpm. A base-apex electrocardiogram was continuously monitored. Images were analysed using Vevo 2100 Workstation software. Parasternal standard, 2D and MM, long and short axis views at the level of the papillary muscles (LAX and SAX view, respectively) were acquired.

Statistical analysis

Expected versus observed frequencies were compared using the χ^2 method.

Adult heart parameters were analysed with unpaired *t*-tests comparing wild type versus Myc-KO and wild type versus heterozygotes separately. Nuclei/myocardium area data were analysed by two-way ANOVA. To compare average percentages of ECFP cells between more than two groups, the Kruskal–Wallis test was used (assuming non-normal distributions). For comparisons of two groups, the Mann–Whitney test was used. All comparisons were made using Prism statistical software.

Single cell RNA-seq analysis

Single cell transcriptome data were downloaded from Gene Expression Omnibus (GSE76118; Li et al., 2016). Cells were classified into Epicardium, Endocardium, Mesenchymal and Cardiomyocytes, as in Li et al., 2016. *Myc* and *Mycn* mRNA expression was analysed for each population and is represented in violin plots.

Acknowledgements

We thank members of the Torres group for stimulating discussions and suggestions. We thank members of the microscopy, bioinformatics and histopathology CNIC units, led by Valeria Caiolfa, Fátima Sánchez-Cabo and Antonio de Molina-Iracheta, respectively, for excellent support and sample processing. We also thank the CNIC Advanced Imaging Unit and the CNIC Animal Facility personnel for their excellent work and support.

Competing interests

The authors declare no competing or financial interests.

Author contributions

Conceptualization: C.V.d.C., M.T.; Methodology: N.M.-M., R.S., C.V.d.C.; Formal analysis: N.M.-M., C.V.d.C.; Investigation: N.M.-M., C.V.d.C.; Resources: T.S.; Writing - original draft: N.M.-M., C.V.d.C., M.T.; Writing - review & editing: T.S., C.V.d.C., M.T.; Supervision: M.T.; Funding acquisition: M.T.

Funding

This work is supported by a grant from the Fondation Leducq [‘Redox Regulation of Cardiomyocyte Renewal’ 17CVD04] and by grants from the Ministerio de Ciencia, Innovación y Universidades [BFU2015-71519-P and RD16/0011/0019 (ISCIII)]. N.M.-M. was supported by a pre-doctoral contract from ‘la Caixa’ Foundation [LACAIXA-SO14]. The CNIC is supported by the Ministerio de Ciencia, Innovación y Universidades and the Pro CNIC Foundation, and is a Severo Ochoa Center of Excellence (SEV-2015-0505).

Supplementary information

Supplementary information available online at <http://dev.biologists.org/lookup/doi/10.1242/dev.170753.supplemental>

References

- Bello Roufai, M., Li, H. and Sun, Z. (2007). Heart-specific inhibition of protooncogene c-myc attenuates cold-induced cardiac hypertrophy. *Gene Ther.* **14**, 1406-1416.
- Charron, J., Malynn, B. A., Fisher, P., Stewart, V., Jeannotte, L., Goff, S. P., Robertson, E. J. and Alt, F. W. (1992). Embryonic lethality in mice homozygous for a targeted disruption of the N-myc gene. *Genes Dev.* **6**, 2248-2257.

- Claveria, C. and Torres, M. (2016). Cell competition: mechanisms and physiological roles. *Annu. Rev. Cell Dev. Biol.* **32**, 411-439.
- Claveria, C., Giovinazzo, G., Sierra, R. and Torres, M. (2013). Myc-driven endogenous cell competition in the early mammalian embryo. *Nature* **500**, 39-44.
- Davis, A. C., Wims, M., Spotts, G. D., Hann, S. R. and Bradley, A. (1993). A null c-myc mutation causes lethality before 10.5 days of gestation in homozygotes and reduced fertility in heterozygous female mice. *Genes Dev.* **7**, 671-682.
- Drenckhahn, J. D., Schwarz, Q. P., Gray, S., Laskowski, A., Kiriazis, H., Ming, Z., Harvey, R. P., Du, X.-J., Thorburn, D. R. and Cox, T. C. (2008). Compensatory growth of healthy cardiac cells in the presence of diseased cells restores tissue homeostasis during heart development. *Dev. Cell* **15**, 521-533.
- Harmelink, C., Peng, Y., DeBenedittis, P., Chen, H., Shou, W. and Jiao, K. (2013). Myocardial Mycn is essential for mouse ventricular wall morphogenesis. *Dev. Biol.* **373**, 53-63.
- Hatton, K. S., Mahon, K., Chin, L., Chiu, F. C., Lee, H. W., Peng, D., Morgenbesser, S. D., Horner, J. and DePinho, R. A. (1996). Expression and activity of L-Myc in normal mouse development. *Mol. Cell. Biol.* **16**, 1794-1804.
- He, C., Hu, H., Braren, R., Fong, S.-Y., Trumpp, A., Carlson, T. R. and Wang, R. A. (2008). c-myc in the hematopoietic lineage is crucial for its angiogenic function in the mouse embryo. *Development* **135**, 2467-2477.
- Huang, C.-Y., Bredemeyer, A. L., Walker, L. M., Bassing, C. H. and Sleckman, B. P. (2008). Dynamic regulation of c-Myc proto-oncogene expression during lymphocyte development revealed by a GFP-c-Myc knock-in mouse. *Eur. J. Immunol.* **38**, 342-349.
- Izumo, S., Nadal-Ginard, B. and Mahdavi, V. (1988). Protooncogene induction and reprogramming of cardiac gene expression produced by pressure overload. *Proc. Natl. Acad. Sci. USA* **85**, 339-343.
- Jackson, T., Allard, M. F., Sreenan, C. M., Doss, L. K., Bishop, S. P. and Swain, J. L. (1990). The c-myc proto-oncogene regulates cardiac development in transgenic mice. *Mol. Cell. Biol.* **10**, 3709-3716.
- Klingberg, A., Hasenberg, A., Ludwig-Portugall, I., Medyukhina, A., Männ, L., Brenzel, A., Engel, D. R., Figge, M. T., Kurts, C. and Gunzer, M. (2017). Fully automated evaluation of total glomerular number and capillary tuft size in nephritic kidneys using lightsheet microscopy. *J. Am. Soc. Nephrol.* **28**, 452-459.
- Knoepfler, P. S., Cheng, P. F. and Eisenman, R. N. (2002). N-myc is essential during neurogenesis for the rapid expansion of progenitor cell populations and the inhibition of neuronal differentiation. *Genes Dev.* **16**, 2699-2712.
- Li, G., Xu, A., Sim, S., Priest, J. R., Tian, X., Khan, T., Quertermous, T., Zhou, B., Tsao, P. S., Quake, S. R. et al. (2016). Transcriptomic profiling maps anatomically patterned subpopulations among single embryonic cardiac cells. *Dev. Cell* **39**, 491-507.
- Machida, N., Brissie, N., Sreenan, C. and Bishop, S. P. (1997). Inhibition of cardiac myocyte division in c-myc transgenic mice. *J. Mol. Cell. Cardiol.* **29**, 1895-1902.
- Malynn, B. A., de Alboran, I. M., O'Hagan, R. C., Bronson, R., Davidson, L., DePinho, R. A. and Alt, F. W. (2000). N-myc can functionally replace c-myc in murine development, cellular growth, and differentiation. *Genes Dev.* **14**, 1390-1399.
- Moens, C. B., Stanton, B. R., Parada, L. F. and Rossant, J. (1993). Defects in heart and lung development in compound heterozygotes for two different targeted mutations at the N-myc locus. *Development* **119**, 485-499.
- Pollack, P. S., Houser, S. R., Budjak, R. and Goldman, B. (1994). c-myc gene expression is localized to the myocyte following hemodynamic overload in vivo. *J. Cell. Biochem.* **54**, 78-84.
- Sawai, S., Shimono, A., Wakamatsu, Y., Palmes, C., Hanaoka, K. and Kondoh, H. (1993). Defects of embryonic organogenesis resulting from targeted disruption of the N-myc gene in the mouse. *Development* **117**, 1445-1455.
- Schneider, M. D., Payne, P. A., Ueno, H., Perryman, M. B. and Roberts, R. (1986). Dissociated expression of c-myc and a fos-related competence gene during cardiac myogenesis. *Mol. Cell. Biol.* **6**, 4140-4143.
- Stanton, B. R., Biben, C., Elefanti, A., Barnett, L., Koentgen, F., Robb, L. and Harvey, R. P. (2002). Efficient Cre-mediated deletion in cardiac progenitor cells conferred by a 3'UTR-ires-Cre allele of the homeobox gene Nkx2-5. *Int. J. Dev. Biol.* **46**, 431-439.
- Stanton, B. R., Perkins, A. S., Tessarollo, L., Sassoon, D. A. and Parada, L. F. (1992). Loss of N-myc function results in embryonic lethality and failure of the epithelial component of the embryo to develop. *Genes Dev.* **6**, 2235-2247.
- Uslu, V. V., Petretich, M., Ruf, S., Langenfeld, K., Fonseca, N. A., Marioni, J. C. and Spitz, F. (2014). Long-range enhancers regulating Myc expression are required for normal facial morphogenesis. *Nat. Genet.* **46**, 753-758.
- Villa del Campo, C., Claveria, C., Sierra, R. and Torres, M. (2014). Cell competition promotes phenotypically silent cardiomyocyte replacement in the mammalian heart. *Cell Reports* **8**, 1741-1751.
- Villa Del Campo, C., Lioux, G., Carmona, R., Sierra, R., Muñoz-Chápuli, R., Claveria, C. and Torres, M. (2016). Myc overexpression enhances of epicardial contribution to the developing heart and promotes extensive expansion of the cardiomyocyte population. *Sci. Rep.* **6**, 35366.
- Xiao, G., Mao, S., Baumgarten, G., Serrano, J., Jordan, M. C., Roos, K. P., Fishbein, M. C. and MacLellan, W. R. (2001). Inducible activation of c-myc in adult myocardium in vivo provokes cardiac myocyte hypertrophy and reactivation of DNA synthesis. *Circ. Res.* **89**, 1122-1129.
- Zhong, W., Mao, S., Tobis, S., Angelis, E., Jordan, M. C., Roos, K. P., Fishbein, M. C., de Alborán, I. M. and MacLellan, W. R. (2006). Hypertrophic growth in cardiac myocytes is mediated by Myc through a Cyclin D2-dependent pathway. *EMBO J.* **25**, 3869-3879.
- Zhou, B., von Gise, A., Ma, Q., Rivera-Feliciano, J. and Pu, W. T. (2008). Nkx2-5- and Isl1-expressing cardiac progenitors contribute to proepicardium. *Biochem. Biophys. Res. Commun.* **375**, 450-453.
- Zimmerman, K. A., Yancopoulos, G. D., Collum, R. G., Smith, R. K., Kohl, N. E., Denis, K. A., Nau, M. M., Witte, O. N., Toran-Allerand, D., Gee, C. E. et al. (1986). Differential expression of myc family genes during murine development. *Nature* **319**, 780-783.

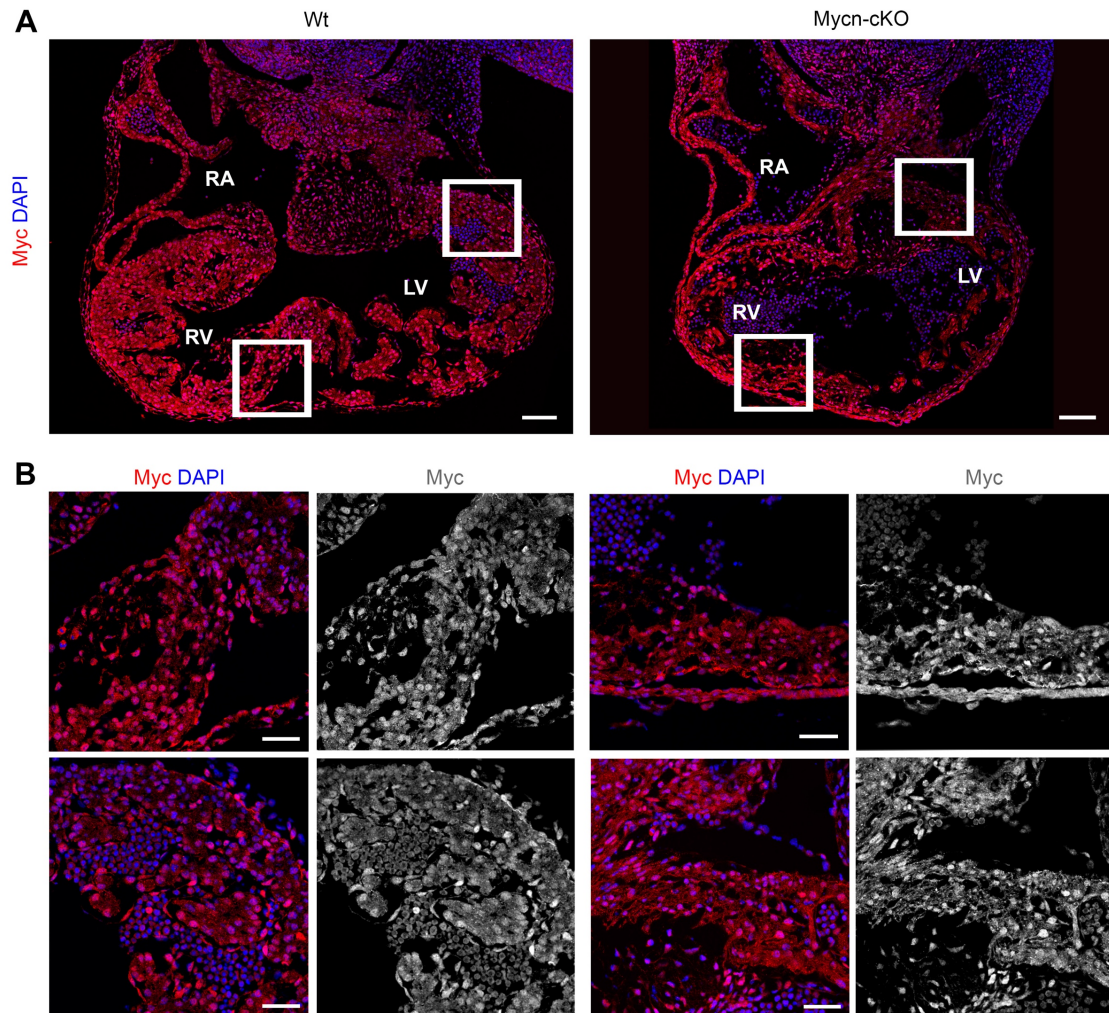


Figure S1. Myc antibody staining in *Mycn*-deficient hearts. **A.** Confocal images showing Myc antibody staining in sections of a E10.5 WT heart (left) and *Mycn*-cKO (right). **B.** Magnification of boxed areas in A. WT heart is shown on left panels and *Mycn*-cKO on right panels. Greyscale images of antibody staining are shown in both cases. Bar 100 μ m in A and 50 μ m in B. LV: Left ventricle, RV: Right ventricle, RA: Right atria, LA: Left atria,

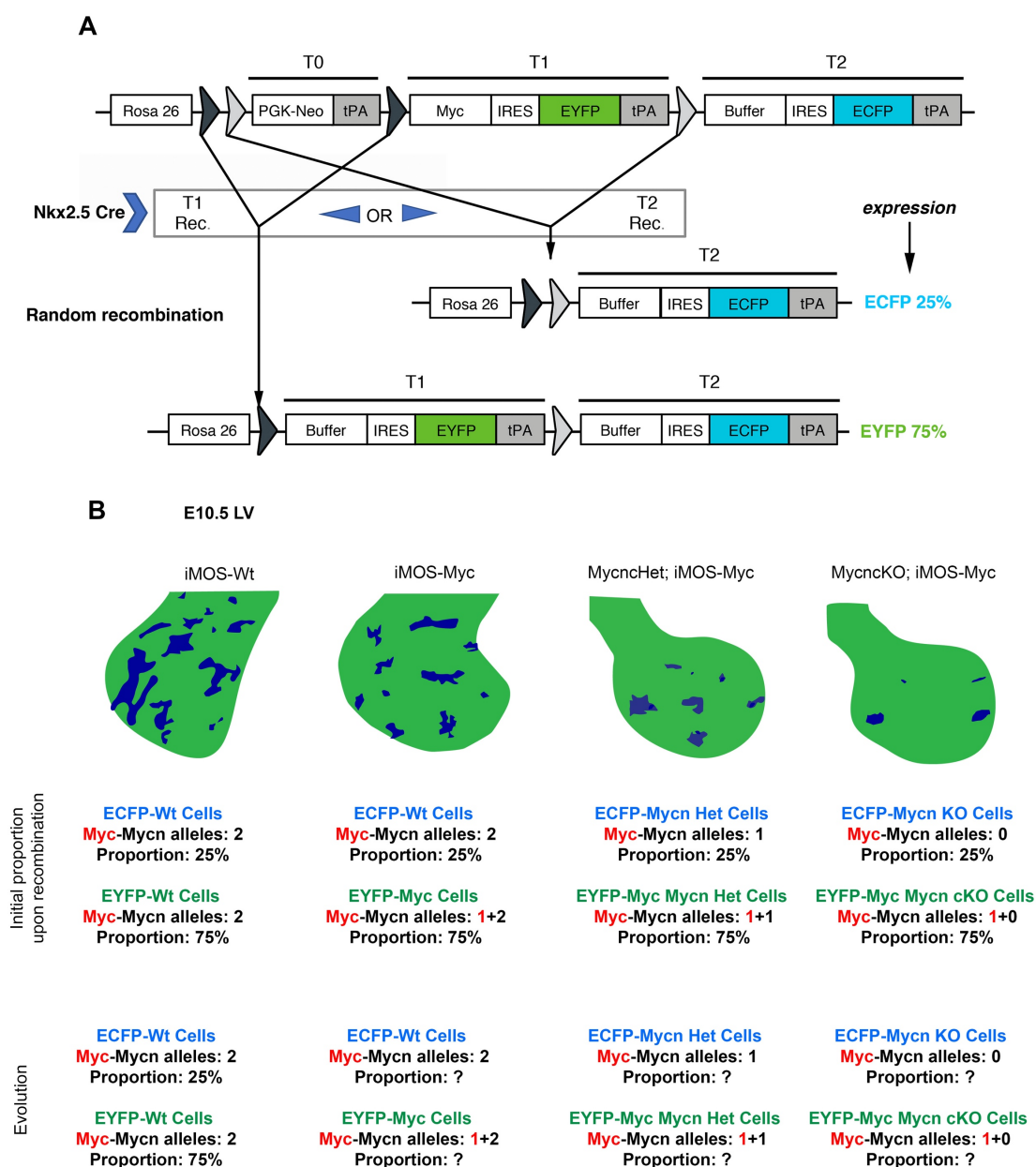


Figure S2. Summary of the iMOS-mosaic system and the different genetic combinations used in this work. A. Schematic of the $iMOS^{T1-Myc}$ allele. The system consists of three cassettes knocked-in to the *Rosa26* locus that can be excised by Cre recombination at random due to two pairs of LoxP sites. When the T0 cassette is excised, T1 is expressed and the cell and its progeny will be labelled in EYFP and overexpress Myc (EYFP-Myc). When T2 recombination takes place both T0 and T1 are excised leading to the expression of T2 (ECFP-WT) in the resulting cell and its progeny. Due to the distances between the lox sites and the Cre efficiency, the proportions of each cell type upon recombination is 75:25 (EYFP:ECFP), as determined experimentally in several tissues. Upon Cre-recombinase exposure, the system thus generates two labelled cell populations at random but reproducible frequencies. **B.** Schematics of E10.5

LV showing the two labelled cell populations in iMOS-WT, iMOS-Myc, MycnHet;iMOS-Myc and MycncKO;iMOS-Myc embryos. Below the images, the proportions and corresponding allele ratio for Myc and Mycn of each cell type is shown. At initial timepoints the relative proportion of EYFP and ECFP proportions is 75:25. In iMOS-Wt this is maintained because no cell population has a competitive advantage over the other. When an imbalance in Myc and Mycn alleles between neighbouring cells is implemented due to the iMOS system and the conditional deletion of Mycn, these proportions vary with developmental progression. Green and blue colours represent the EYFP and ECFP cell populations, respectively.

Table S1. Observed and expected frequencies of adult mice of the different genotypes

Genotype	Adult mice	Observed frequency	Expected frequency
WT	20	0.266	0.25
cHet-Myc	38	0.506	0.50
cKO-Myc	18	0.240	0.25